PHYSICAL REVIEW A **87**, 031404(R) (2013)

Electron dynamics in the ground state of a laser-generated carbon atom

Hannes Hultgren,[1] Mikael Eklund,[1] Dag Hanstorp,[2] and Igor Yu. Kiyan[1,*]
[1]*Physikalisches Institut, Albert-Ludwigs-Universität, 79104 Freiburg, Germany*
[2]*Department of Physics, University of Gothenburg, SE-412 96 Gothenburg, Sweden*
(Received 20 September 2012; published 29 March 2013)

We present a real-time observation of electron motion in the ground state of the carbon atom. A wave packet is created in the ground triplet state of the atom via photodetachment of its negative ion in a strong laser field. Its dynamics is probed using the selectivity of strong-field ionization to orbital alignment in combination with an electron-imaging technique. A strong temporal modulation in the photoelectron yield at high kinetic energies is observed, which reveals a periodic motion of the electron cloud in the atom.

DOI: 10.1103/PhysRevA.87.031404 PACS number(s): 32.80.Rm, 32.80.Gc, 78.47.jm

The study of electron dynamics in real time in atoms and molecules represents a topic of fundamental interest. An ultimate goal is to monitor and achieve control over chemical reactions at atomic dimensions [1]. The advances in femto- and attosecond laser technology provide a powerful tool to resolve the electronic motion on the ultrashort time scale [2,3]. A wide range of studies focused on the electron dynamics in excited systems, where a coherent superposition of eigenstates was created by means of a phototransition from the ground state of the parent atom or molecule. Recently, an approach to create a coherent wave packet in the *ground* state of a laser-generated positive ion was theoretically described [4] and experimentally implemented [5,6]. This approach is based on the removal of one electron from the atomic or molecular valence shell by means of strong-field ionization in a short laser pulse, which leads to the creation of a localized hole in the electron density distribution of the residual core. It can be applied to quantum systems that initially possess two or more valence electrons having a nonzero angular momentum. In the present work we develop this approach to study electron dynamics in the ground state of a neutral atom. This subject is of particular interest, since many common chemical reactions occurring in nature involve interactions of neutral particles.

The possibility to create a localized hole of electron density in the valence shell is given by the fact that electron emission in a strong linearly polarized laser field is dependent on the orientation of the electron orbital, i.e., on the magnetic quantum number m_ℓ of the initial state. The angular-momentum quantization axis is provided by the field polarization. Orbitals with $m_\ell = 0$ display emission rates orders of magnitude higher than orbitals with $m_\ell \neq 0$ [7,8]. Hence, after the laser pulse the ionized atomic system is left with a hole in the electron density distribution localized along the laser polarization direction. This constitutes the orbital alignment effect discussed in Refs. [9–12].

From the theoretical point of view, the spatially confined hole is created due to a coherent superposition of the spin-orbit components of the ground state of the core. For example, positive ions generated via ionization of noble gas atoms can be left either in the $p^{-1}_{j=3/2}$ or $p^{-1}_{j=1/2}$ manifolds associated with a hole in the valence p shell. In order to populate these manifolds coherently, the ionization process is required to be faster than the spin-orbit period of the ground state [4]. Since the wave packet is composed of states having different energies, the created hole is nonstationary and moves around the core [5]. Different methods were used to monitor the electronic motion in the laser-generated positive ions. These include the transient absorption spectroscopy with the use of isolated attosecond extreme-ultraviolet pulses [5], and the ionization-probe spectroscopy involving measurements of the recoil momentum of the doubly charged ion and the total ionization yield [6].

Until now the study of orbital alignment and its time evolution has been restricted to the case of ionization of noble gas atoms [5,6,9–12]. Extension of this study to other quantum systems, such as negative ions, is of great interest. Angular electron correlations were shown in Ref. [6] to play a major role in the formation of the electron-density hole. Therefore, one should expect the alignment effect to be more pronounced in the process of photodetachment of negative ions, since electron correlations are crucial in the formation of their electronic structure [13]. The alignment effect was considered in our previous experiment on double detachment of halogen negative ions in the sequential regime [14]. In this regime, the laser-generated atoms represent a target for the subsequent ionization step and, thus, their orbital alignment should manifest itself in the ionization yield. However, investigation of the alignment dynamics was precluded in the previous work by the fact that a single laser pulse was used to drive both the detachment and the ionization steps.

In the present work, we develop a method to explore the orbital alignment and its dynamics following the photodetachment event. We probe the electron density of the generated atom by ionizing it with a second strong laser pulse applied at a variable time delay. The difference between our approach and studies on noble gas atoms is that we record angle-resolved spectra of ionized electrons instead of integrated yields. As discussed above, the strong field primarily ionizes the spatial portion of the electron density which is oriented along the polarization axis. By employing an electron imaging technique, we project this portion onto a position-sensitive detector. This enables us to visualize the electron density aligned along the polarization axis of the probe pulse and to monitor the motion of the electron cloud

*Current address: Helmholtz-Zentrum für Materialien und Energie, Albert-Einstein-Str. 15, 12489 Berlin, Germany.

in real time. We apply this method to investigate the electron dynamics in the electronic ground state of the carbon atom. The possibility of its control is of special interest because this element is involved in many important chemical reactions occurring in nature. Since the carbon negative ion possesses an open outer shell, the formation of the electron-density hole involves coherent population of three spin-orbit components of the ground atomic state. This complexity of the hole formation will be addressed in our discussion.

The experiment was performed using an electron imaging spectrometer (EIS) and a laser system that generated a pair of short pulses of 100-fs duration in the infrared wavelength region. The linearly polarized idler (2055 nm) and signal (1310 nm) outputs from an optical parametric amplifier, pumped with a mode-locked Ti:sapphire laser, were used as the pump and probe beams, respectively. The laser beams were spatially overlapped in the region of interaction with negative ions. The peak intensities of 8×10^{13} and 4×10^{14} W/cm^2 for the pump and probe pulses, respectively, were reached by focusing the beams. Their focal positions along the beam propagation direction were made to coincide by adjusting the divergence of the pump beam with the use of a telescope. The optical setup enabled us to vary the time delay between pulses and control their polarization axes. The zero time delay between pulses was defined by optimizing the yield of their sum-frequency generation in a BBO crystal. The accuracy of setting the time delay to zero was of the order of 50 fs. Negative carbon ions were created in a sputter ion source, accelerated, and subsequently mass selected in a Wien filter before being intersected with the two laser beams inside the EIS. By applying an electrostatic field, electrons emitted in both detachment and ionization steps were projected together onto the position-sensitive detector of the EIS. The EIS does not reveal whether the electrons are generated by the pump pulse or the probe pulse. In order to isolate the ionization yield, photoelectron spectra generated by the pump pulse alone were subtracted from the images. More details on the ion beam apparatus and the EIS can be found in Ref. [15].

The ground quartet $^4S_{3/2}$ state of C^- possesses three p electrons having parallel spins but different magnetic quantum numbers, $m_\ell = -1, 0, +1$. Since the strong field detaches primarily the $m_\ell = 0$ electron, this orbital is depleted after the detachment step and the atom acquires a high degree of orbital alignment. The pump laser generates the carbon atoms in the ^3P ground state. It represents the only detachment channel since spin conservation does not allow transitions to the ^1D and ^1S atomic states, having the same $2p^2$ configuration (see Fig. 1 for the diagram of energy levels of C^- and C). The wave packet of spin-orbit components of the ^3P ground state with the localized hole in the $m_\ell = 0$ orbital is populated coherently. Indeed, the shortest spin-orbit period derived from the energy splitting of the $J = 0$ and $J = 2$ components is 769 fs. This period is one order of magnitude larger than the rise time of the leading front of the pump pulse, where the photodetachment process generates most of the atoms. According to our simulations based on the strong-field approximation (SFA), this time interval extends over approximately 50 fs. A detailed description of the SFA simulation routine that includes the integration of the electron yield over the spatiotemporal intensity distribution in the laser focus as well as the saturation effect can be found in Ref. [18]. While the intensity of the pump pulse is sufficiently high to saturate the photodetachment process at the leading edge of the pulse, our simulations show that its contribution to ionization of the residual atoms is negligible. This is due to the low pump photon energy of 0.60 eV, which requires 18 photons to overcome the ionization threshold of carbon.

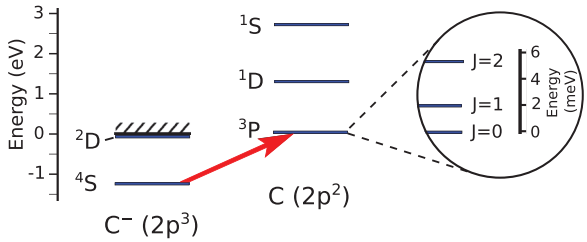

FIG. 1. (Color online) Energy levels of C^- [16] and its parent atom in the $2p^2$ ground-state configuration [17]. The arrow denotes photodetachment with the formation of the carbon atom in the ^3P state.

After a variable time delay, the laser-generated carbon atoms were exposed to the linearly polarized probe pulse of higher photon energy and higher intensity. The probe pulse ionized atoms with high efficiency. According to the semiclassical description, strong-field ionization generates electrons with kinetic energies up to twice the ponderomotive energy [19]. Under our experimental conditions, this cutoff corresponds to approximately 128 eV, which is significantly larger than the probe photon energy of 0.95 eV. While intensities from zero to the peak value are available in the laser focus, it is the high-energy part of the photoelectron spectrum that reveals the contribution of high intensities to the ionization yield. In this region of the spectrum, the angular distribution of emitted electrons is narrow, forming two electron jets along the laser polarization axis [14]. This reflects the fact that a strong external field preferentially detaches the part of the electron cloud that is localized along the electric field vector, consistent with the above discussion of the m_ℓ-dependency of the ionization rate. Thus, by imaging the photoelectron yield in the high-energy jets we directly probe the electron density in the bound state along the laser polarization axis. This was performed in our experiment by projecting the emitted electrons onto the position-sensitive detector of the EIS while keeping the probe polarization parallel to the detector plane.

While the pump polarization defines the axis of orbital alignment created initially in the carbon atom, the probe pulse monitors the electron density distribution along its own polarization axis. The ionization yield in the jets was observed to be dependent on the hole-density state, controlled by the pump-probe delay and by the orientation of the pump polarization with respect to the probe polarization axis. In order to reveal the wave packet dynamics with a higher signal-to-background contrast, at each time delay we subtracted the image recorded with the pump polarization being parallel to the probe polarization from the image recorded with perpendicular polarization directions.

Figure 2 shows three representative images recorded at pump-probe time delays of 2000, 2300, and 2600 fs, respectively. The images display the difference in angle resolved

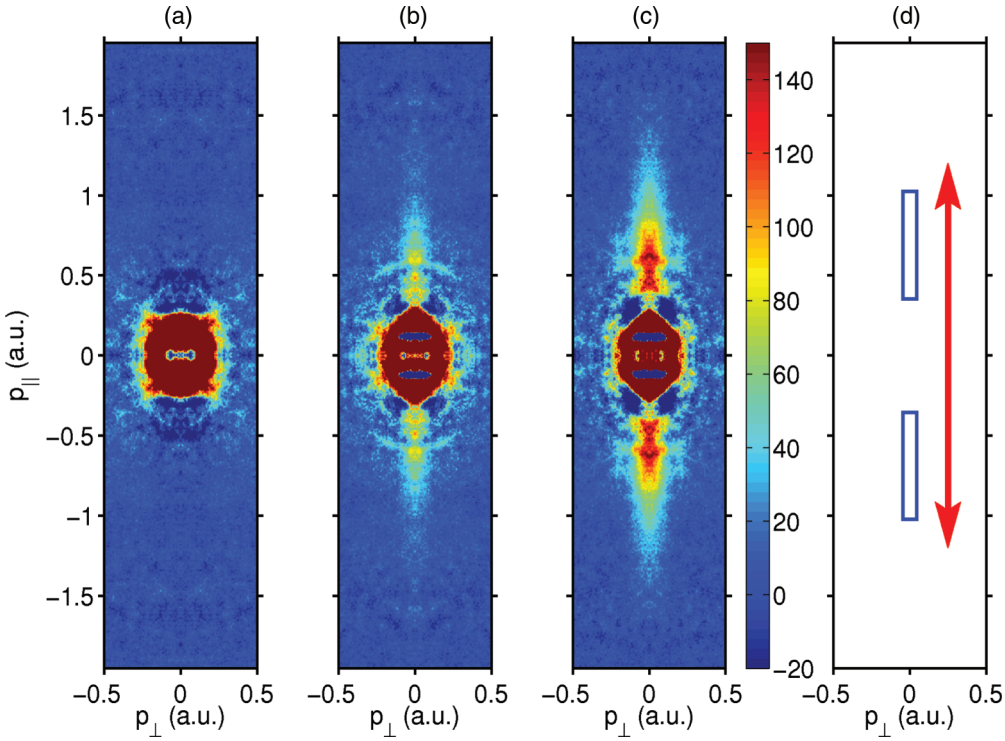

FIG. 2. (Color online) Images of photoelectrons recorded at pump-probe time delays of 2000 fs (a), 2300 fs (b), and 2600 fs (c). $p_\parallel$ and $p_\perp$ denote the electron momentum components parallel and perpendicular to the polarization axis of the probe beam, represented by the arrow in (d). The two rectangles shown in (d) represent the area over which the electron yield was integrated to obtain the data shown in Fig. 3.

momentum distributions of photoelectrons recorded with different orientations of the pump polarization. The electron momentum is proportional to the distance from the center of the image, and the vertical arrow in Fig. 2(d) indicates the direction of the probe laser polarization. A momentum of 1.5 a.u. corresponds to the absorption of 45 photons of the probe beam. The main differences in the presented images are the number of high-energy electrons emitted along the laser polarization, seen as two vertically oriented jets. The signal of low energy electrons in the center of the images is primarily due to photodetachment by the probe beam of negative ions that survived the pump pulse.

The experimental results presented in Fig. 2 can be directly understood from the time evolution of the created electronic wave packet. Following the pump pulse, the electron hole in the valence shell of the carbon atom starts its evolution. Its density distribution interchanges between being localized along and perpendicular to the quantization axis defined by the pump pulse polarization. When the hole turns to be localized along the polarization axis of the probe beam, there are no high-energy electrons produced because of the low electron density along the probe field vector. The image shown in Fig. 2(a) corresponds to such a case. In Fig. 2(c), on the other hand, the hole has moved to be localized around the horizontal plane, i.e., at 90° with respect to the probe polarization. At this stage there is a high electron density along the probe laser polarization, yielding a strong signal of high-energy electrons. A significant dependence on the pump-probe delay time in the amount of ionized high-energy electrons, therefore, appears in Figs. 2(a)–2(c), manifested as a change in the intensity of the electron jets.

Figure 3 displays the time dependency $S(t)$ of the amount of high-energy electrons within the area of the two rectangles shown in Fig. 2(d). The electron yield was normalized as

$$S(t) = \frac{S_\perp(t) - S_\parallel(t)}{S_\perp(t) + S_\parallel(t)},$$

where $S_\parallel(t)$ and $S_\perp(t)$ represent the signal in the jets recorded with the pump and probe polarizations being parallel and perpendicular, respectively. The large modulation of S manifests a strong orbital alignment achieved in the process of photodetachment. It was anticipated in view of the fundamental role of electron correlations in the formation of the electronic structure of negative ions.

The time evolution can be described in terms of a quantum beat between the three fine structure components of the ground state of the carbon atom. The time period τ of the beat of two coherent states is given by $\tau = h/\Delta E$, where ΔE is the

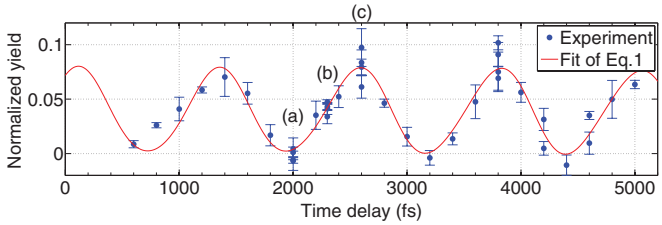

FIG. 3. (Color online) The normalized yield of high-energy electrons emitted in the ionization step plotted as a function of the time delay between the pump and probe pulses. The solid line represents the fit result of Eq. (1) to the data set. Images shown in Fig. 2 are associated to the data points denoted by (a), (b), and (c).

TABLE I. Fine structure splittings (ΔE_{FS}), calculated beat periods (τ_{cal}), measured beat periods (τ_{exp}), and amplitudes (β) of the quantum beats. The uncertainties represent one standard deviation.

Beat	ΔE_{FS} (meV)	τ_{cal} (fs)	τ_{exp} (fs)	β (10^{-3})
J_{01}	2.03	2034	1931 ± 1456	0.417 ± 2.879
J_{02}	5.38	769	636.8 ± 22.7	3.105 ± 2.732
J_{12}	3.35	1235	1229 ± 17	38.53 ± 2.71

energy spacing between the states involved, and h is the Planck constant. In our case, there are three coherently populated fine structure components, which give rise to three possible beat periods represented by τ_1 (J = 2,1), τ_2 (J = 2,0), and τ_3 (J = 1,0). A phenomenological function

$$f(t) = \beta_0 + \sum_{i=1}^{3} \beta_i \cos\left[\frac{2\pi}{\tau_i}(t - t_0)\right], \qquad (1)$$

containing the sum of three harmonic functions is, therefore, fitted to the data set, with β_0, β_i, τ_i, and t_0 being the fit parameters. Here, β_0 represents a constant background and β_i are the amplitudes of oscillations at the individual beat frequencies. While the time delay is measured between the maxima of the pump and probe pulses, we cannot experimentally determine the instance at the leading front of the pump pulse where the detachment process is saturated, nor the instance during the probe pulse where the ionization yield is maximum. Because of this uncertainty and the limited accuracy in the determination of the zero time delay, the fit parameter t_0 is introduced in Eq. (1).

The results of the fit are shown in Table I together with the oscillation periods calculated using the tabulated values of the fine structure splitting ΔE_{FS} [17]. The experiment covers more than three oscillations of the electron-density hole. The results demonstrate that the hole-density evolution in the ^3P state is mainly determined by the beat J_{12} between the $J = 1$ and $J = 2$ levels. This can be explained by considering that the spin-orbit components are populated according to their statistical weights $2J + 1$. By comparing the experimentally determined oscillation periods with calculated values, we find that for the main beat J_{12} the measured value of 1229 ± 17 fs is in excellent agreement with the calculated value of 1235 fs. For the J_{02} oscillation, the measured amplitude is of the order of one standard deviation. The J_{01} amplitude is not statistically significant.

In conclusion, we present a method to initiate and to monitor in real time electron motion in the ground state of a neutral atom. It opens a wide range of applications, where coherent control over a process can be achieved by preparing the reactive atom in its ground state with a desirable electron density distribution. Such control needs that the electron cloud remains steady during the process. The intrinsic time scale of the electron motion is found to be determined by the beat between the two fine-structure components of the ground state with the highest statistical weights. For light elements, such as the carbon atom considered in this work, the beat period lies in the picosecond range. Thus, the prepared electron density distribution can be preserved while the atom undergoes a chemical reaction. We would like to emphasize that the present study addresses control of electron dynamics in a *neutral* atomic system, and this work represents a big advance regarding that interactions of neutral particles constitute many reactions occurring in nature. Further development of our method to control electron dynamics in neutral molecules is of great importance.

No sign of decoherence of the wave packet is visible within the experimental time window. The time scale of decoherence and its possible mechanisms represent an interesting subject for further studies. We expect that the collisional interaction of an orbitally aligned atom with the environment is the major source of decoherence compared to internal mechanisms such as radiative decay of a higher-lying spin-orbit component. Since a dilute target in the form of a negative ion beam was used in the present experiment, an extension of this study to more dense media containing negative ions is of great interest.

The authors greatly appreciate enlightening discussions with Hanspeter Helm. This work was funded by the Deutsche Forschungsgemeinschaft (DFG), Grant No. KI 865/3-1. D.H. acknowledges support by the Swedish Research council, and M.E. acknowledges support by the EU-ITN Network ICONIC 238671.

[1] M. Wollenhaupt and T. Baumert, Faraday Discuss. **153**, 9 (2011).
[2] G. Sansone *et al.*, Nature (London) **465**, 763 (2010).
[3] M. Uiberacker *et al.*, Nature (London) **446**, 627 (2007).
[4] N. Rohringer and R. Santra, Phys. Rev. A **79**, 053402 (2009).
[5] E. Goulielmakis *et al.*, Nature (London) **466**, 739 (2010).
[6] A. Fleischer *et al.*, Phys. Rev. Lett. **107**, 113003 (2011).
[7] M. Ammosov, N. Delone, and V. Krainov, Sov. Phys. JETP **64**, 1191 (1986).
[8] M. V. Frolov, N. L. Manakov, E. A. Pronin, and A. F. Starace, Phys. Rev. Lett. **91**, 053003 (2003).
[9] L. Young *et al.*, Phys. Rev. Lett. **97**, 083601 (2006).
[10] Z.-H. Loh *et al.*, Phys. Rev. Lett. **98**, 143601 (2007).
[11] S. H. Southworth *et al.*, Phys. Rev. A **76**, 043421 (2007).
[12] C. Höhr *et al.*, Phys. Rev. A **75**, 011403 (2007).
[13] H. S. W. Massey, *Negative Ions*, 3rd ed. (Cambridge University Press, Cambridge, 1976).
[14] B. Bergues and I. Yu. Kiyan, Phys. Rev. Lett. **100**, 143004 (2008).
[15] R. Reichle, H. Helm, and I. Yu. Kiyan, Phys. Rev. A **68**, 063404 (2003).
[16] H. Hotop and W. C. Lineberger, J. Phys. Chem. Ref. Data **14**, 731 (1985).
[17] A. Kramida *et al.*, NIST Atomic Spectra Database, version 5.0, http://physics.nist.gov/asd (2013).
[18] B. Bergues, Z. Ansari, D. Hanstorp, and I. Yu. Kiyan, Phys. Rev. A **75**, 063415 (2007).
[19] G. G. Paulus *et al.*, J. Phys. B **27**, L703 (1994).